Cell

Depolymerizing Kinesins Kip3 and MCAK Shape Cellular Microtubule Architecture by Differential Control of Catastrophe

Melissa K. Gardner,[1,2,3] Marija Zanic,[2,3] Christopher Gell,[2] Volker Bormuth,[2] and Jonathon Howard[2,*]
[1]Department of Genetics, Cell Biology, and Development, University of Minnesota, Minneapolis, MN 55455, USA
[2]Max Planck Institute of Molecular Cell Biology and Genetics, 01307 Dresden, Germany
[3]These authors contributed equally to this work
*Correspondence: howard@mpi-cbg.de
DOI 10.1016/j.cell.2011.10.037

SUMMARY

Microtubules are dynamic filaments whose ends alternate between periods of slow growth and rapid shortening as they explore intracellular space and move organelles. A key question is how regulatory proteins modulate catastrophe, the conversion from growth to shortening. To study this process, we reconstituted microtubule dynamics in the absence and presence of the kinesin-8 Kip3 and the kinesin-13 MCAK. Surprisingly, we found that, even in the absence of the kinesins, the microtubule catastrophe frequency depends on the age of the microtubule, indicating that catastrophe is a multi-step process. Kip3 slowed microtubule growth in a length-dependent manner and increased the rate of aging. In contrast, MCAK eliminated the aging process. Thus, both kinesins are catastrophe factors; Kip3 mediates fine control of microtubule length by narrowing the distribution of maximum lengths prior to catastrophe, whereas MCAK promotes rapid restructuring of the microtubule cytoskeleton by making catastrophe a first-order random process.

INTRODUCTION

Microtubules are highly dynamic polymeric filaments for which the protein subunit tubulin rapidly exchanges with the soluble pool. Filament turnover is essential for many cellular processes such as cell motility and mitosis. Assembly and disassembly of filaments can generate force (Dogterom et al., 2005), and the balance between growth and disassembly dynamically determines the distribution of filament lengths. How filament growth and shrinkage are regulated by nucleotide hydrolysis and by regulatory proteins is a central question in cell biology.

Microtubules turn over primarily by a process called dynamic instability. This process involves gain and loss of subunits at one end only: assembly at the plus end alternates stochastically with disassembly at the same end (Mitchison and Kirschner, 1984). The other end of the microtubule (the minus end) is usually stabilized at the microtubule-organizing center or at the centrosome and participates to a lesser extent in subunit exchange. The sudden random transition at the plus end between relatively slow growth and rapid shortening is termed catastrophe. Despite intense study for many years, the catastrophe mechanism and its regulation by so-called catastrophe factors are still poorly understood.

Catastrophe is thought to occur as a result of the loss of a stabilizing GTP-tubulin cap at the plus end of the microtubule. This GTP-cap model is supported by the following evidence: (1) microtubule growth involves addition of GTP-tubulin from solution, (2) there is a lag between subunit addition and GTP hydrolysis (Carlier et al., 1984; Nogales and Wang, 2006; Nogales et al., 1998), (3) tubulin subunits bound to the slowly hydrolyzable GTP analog GMPCPP dissociate slowly from the microtubule end (Hyman et al., 1992) and, when added to the ends of GDP-microtubules, prevent depolymerization (Mickey and Howard, 1995), (4) GDP-tubulin microtubules depolymerize rapidly following dilution of soluble tubulin or after microtubule severing (Walker et al., 1989, 1991), and (5) an antibody raised to GTPγS-tubulin, which also binds GMPCPP microtubules, preferentially labels the plus ends of microtubules (Dimitrov et al., 2008), similar to EB1 (Maurer et al., 2011; Zanic et al., 2009). However, the GTP cap has never been visualized on a dynamic, growing microtubule and thus remains hypothetical. Whereas a single GTP tubulin at the end of each of the 13 protofilaments that make up the microtubule is sufficient for stabilization (Caplow and Shanks, 1996; Drechsel and Kirschner, 1994), it is not known how many protofilaments need to become uncapped before catastrophe occurs or even whether loss of the presumed GTP cap is necessary for catastrophe. Furthermore, the mechanism by which microtubule-binding proteins influence catastrophe rates and whether or how they influence the properties of the cap are not known.

In this work, we asked how depolymerizing kinesins influence microtubule dynamics. In cells, both kinesin-8 and kinesin-13 are catastrophe factors that dramatically affect the number, distribution, and lengths of microtubules. Depletion of the kinesin-13 MCAK in mitotic egg extracts decreases the catastrophe rate and increases mitotic spindle length (Desai et al., 1999; Tournebize et al., 2000; Walczak et al., 1996). In *Drosophila* cells or embryos, RNAi or antibodies against kinesin-13 increase spindle

length (Goshima et al., 2005; Rogers et al., 2004) and increase the lengths of astral microtubules (Goshima et al., 2005). Conversely, in vivo overexpression of MCAK results in loss of spindle microtubules (Maney et al., 1998) and increased catastrophe frequency (Kline-Smith and Walczak, 2002). Kinesin-8 is a catastrophe factor in budding yeast (Desai et al., 1999; Gardner et al., 2008; Gupta et al., 2006) and fission yeast (Tischer et al., 2009), where it plays a role in spindle positioning. Kinesin-8 deletion mutants in budding yeast have aberrant chromosome positioning (Gardner et al., 2008; Gupta et al., 2006; Wargacki et al., 2010), and RNAi of the Kif18A kinesin-8 in mammalian cells leads to large fluctuations in chromosome position during metaphase, suggesting that Kif18A affects individual microtubule dynamics within kinetochore fibers (Mayr et al., 2007; Stumpff et al., 2008). These phenotypes are all consistent with kinesin-8 and -13 being catastrophe factors.

Experiments with purified proteins show that both kinesin-8 (Kip3, Kif18A) and kinesin-13 (MCAK) can depolymerize microtubules stabilized by taxol or GMPCPP (Desai et al., 1999; Gupta et al., 2006; Helenius et al., 2006; Hunter et al., 2003; Mayr et al., 2007; Varga et al., 2006, 2009). Based on the assumption that GMPCPP-tubulin is a model for GTP-tubulin, it has been suggested that the mechanism underlying the increase in catastrophe rate observed in vivo is depolymerization of the GTP cap (Gupta et al., 2006; Varga et al., 2006, 2009). However, it has not been shown that purified kinesin-8 increases the catastrophe rate of microtubules, nor has kinesin-13 been shown to promote catastrophes of dynamic microtubules on its own, though it does promote catastrophes in the presence of other proteins such as XMAP215 (Kinoshita et al., 2002) and EB1 (Montenegro Gouveia et al., 2010) and destabilizes microtubules polymerized from purified HeLa cell tubulin (Newton et al., 2004). The goal of this study was to determine whether Kip3 and/or MCAK are catastrophe factors in vitro and, if so, what the mechanism is.

One expectation that we had before starting these experiments was that Kip3 might be a length-dependent catastrophe factor. This expectation was based on our earlier finding that Kip3 depolymerizes long microtubules faster than short ones due to the so-called ''antenna'' effect: the longer the microtubule, the more motors land on it, and therefore, because Kip3 is a highly processive motor, more motors reach the plus end of longer microtubules, where they remove tubulin dimers (Varga et al., 2006, 2009). We therefore hypothesized that the longer the microtubule, the more labile the cap, and therefore the higher the catastrophe rate. In order to test this hypothesis, we needed to measure carefully the kinetics of microtubule catastrophes in the absence of kinesins. Surprisingly, we found that, even in the absence of kinesins, microtubules have a length-dependent catastrophe frequency. Therefore, we begin the paper by describing catastrophes in tubulin alone, and because the results were surprising and have unexpected and interesting implications on the nature of the GTP cap and the mechanism of catastrophe, we have included several control experiments so that we can be sure of the ''baseline.'' We then tested the influence of the depolymerizing kinesins on catastrophes and, in a further surprise, found that they influenced catastrophes by quite different mechanisms.

RESULTS

Catastrophes Visualized by TIRF Microscopy

To study catastrophes of dynamic microtubules, we assembled GTP-tubulin labeled with green Alexa-488 (Invitrogen Corporation) onto red GMPCPP-tubulin seeds attached to a coverslip in a total internal reflection fluorescence (TIRF) microscope assay (Gell et al., 2010) (Figure 1A). A slice through the microtubule image was taken in each frame of the time-lapse movie, and the slices were displayed one under another to generate a kymograph. Catastrophes were clearly observed, and both the catastrophe time and the catastrophe length were independently recorded for each event (Figure 1A). The catastrophe time, also called the microtubule lifetime, is the elapsed time during which a microtubule grows prior to catastrophe. This is the microtubule's age at catastrophe. Under the conditions of our assay, rescue events were not observed.

We measured the catastrophe time of 692 microtubules at a free GTP-tubulin concentration of 12 μM. The 692 times were plotted as a cumulative distribution curve (Figure 1B, blue): the catastrophe events were ordered from shortest to longest time to catastrophe, and each point on the graph corresponds to the time (x axis) and event number normalized by the total number of events (y axis). For each time, the y axis value of the cumulative distribution corresponds to the fraction of microtubules that underwent catastrophe prior to that time. The distribution has the value zero at time zero (corresponding to initiation of growth off the seed) and approaches one for large times.

Microtubule Catastrophe Requires Multiple Steps

It is widely assumed (but see Odde et al., 1995, 1996; Stepanova et al., 2010) that catastrophe is a first-order process that is described by a single rate constant (Howard, 2001; Phillips et al., 2008). According to this assumption, the catastrophe rate is independent of the microtubule age, and therefore, the rate constant can be estimated by dividing the number of catastrophe events by the total microtubule growth time. If this assumption is correct, then the cumulative distribution should increase linearly for short times. However, the cumulative distribution shows a clear nonlinearity at early time points (Figure 1B, inset, blue dots). Furthermore, the cumulative distribution falls well below the predicted constant catastrophe rate line (Figure 1B, inset, red line), indicating that there is a paucity of catastrophes at short times. The ''missing'' catastrophes cannot be accounted for by failure to detect the short microtubules in our assay: microtubules of age 45 s have lengths ~675 nm, corresponding to 10 pixels, and are easily detected (the red line is shifted by 45 s to account conservatively for possible missing events at short times), and yet there remains a large difference between the single-step model and the data, as shown by the black double arrow in Figure 1B (inset) (also Figure S1 available online). We conclude that younger microtubules have a lower catastrophe rate than older microtubules. Thus, our data are not consistent with catastrophe being a single transition between a growing phase and a shortening phase. This suggests that catastrophe is a multistep process (Figure 1C).

To test quantitatively whether our catastrophe time data are consistent with a single-step catastrophe model, we used the

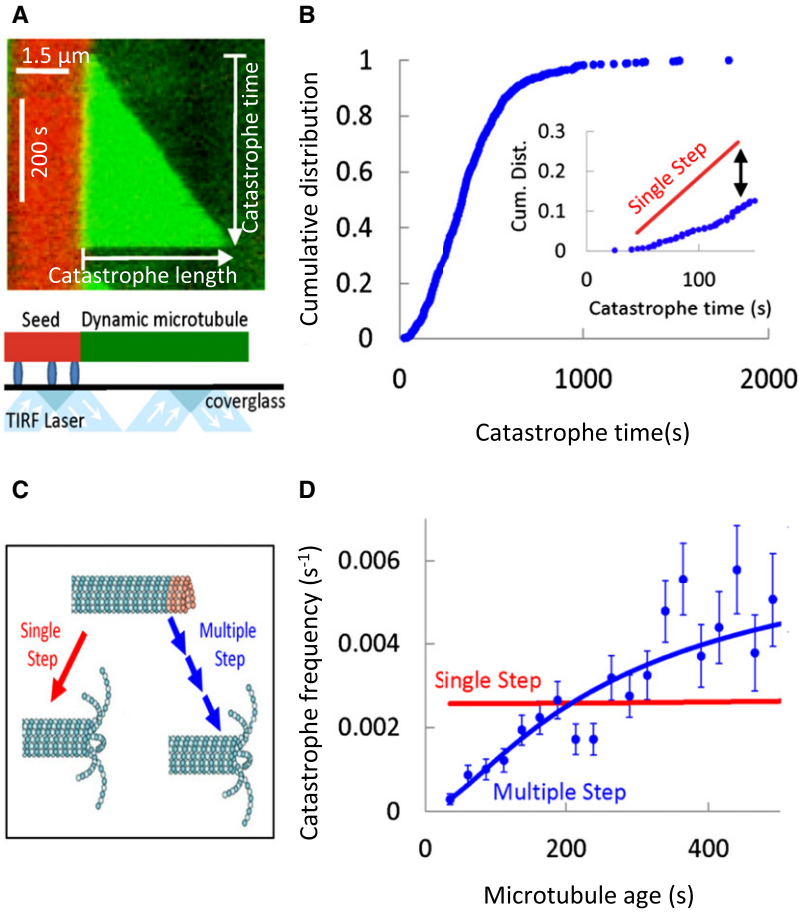

Figure 1. Catastrophe of In Vitro Microtubules Is a Multistep Process

(A) Kymograph showing the catastrophe of a green microtubule extension growing from a red seed.

(B) The experimentally observed distribution of catastrophe times (blue dots) is represented using a cumulative distribution plot. The catastrophe distribution at short times, though expected to be linear for a single-step stochastic process (inset, red line), is nonlinear due to fewer observed short time catastrophe events than predicted by a single-step process (black double arrow). The red line is offset by 45 s to represent a conservative estimate of short-duration, missed catastrophes.

(C) Catastrophe has been considered to be a single-step process (left, red), in which a single stochastic catastrophe-promoting event is equally likely at any moment in time. Alternatively, catastrophe could be a multistep process (right, blue), in which several features required for catastrophe are remembered over time.

(D) The catastrophe frequency increases with microtubule age (blue dots), consistent with a multistep catastrophe process and inconsistent with a single-step process (red line). Error bars represent SE.

See also Figures S1 and S2.

cumulative distribution, $F(t)$, to measure the time-dependent catastrophe frequency, $f_{\pm}(t)$, as a function of microtubule age, t, according to:

$$f_{\pm}(t) = \frac{dF(t)/dt}{1 - F(t)}. \quad (1)$$

The catastrophe frequency represents the ratio of the number of catastrophes observed at age t to the total number of microtubules that reached age t. The above relationship assumes that there are no rescues, as was the case under these conditions. As shown in Figure 1D (blue markers), the catastrophe frequency increased from near zero for young microtubules and tended toward a saturation value of $\approx 0.005\ s^{-1}$ for older microtubules. It is clear that a single-step, first-order process described by a constant catastrophe frequency (Figure 1D, red line) is inconsistent with our data.

A catastrophe frequency that increases from zero and saturates at long times is indicative of a multistep aging process. Such a process has memory: a number of independent events must occur before catastrophe, and each of these events is remembered, such that the microtubule end becomes less stable over time.

A commonly used distribution that describes a multistep process with n equal random steps is the gamma distribution (Rice, 1995). The assumption of equal steps minimizes the variance of the distribution, so the gamma distribution gives the lower limit on the number of steps in a multistep process. The gamma distribution has been widely used to model waiting times (Rice, 1995) and has been previously used to describe microtubule catastrophes (Odde et al., 1995; 1996).

The gamma distribution as applied to microtubule catastrophe is characterized by two parameters: a step parameter n, which describes the minimum number of steps that are required to produce a catastrophe, and a rate parameter, r, which describes the rate of occurrence of each step (Figure S2). A single-step model is a special case with step parameter n = 1 and in which microtubule catastrophe does not depend on age. Using these parameters, the predicted number of catastrophe events at time t (the probability density function) is:

$$\frac{dF_n(t)}{dt} = \frac{r^n t^{n-1} e^{-rt}}{\Gamma(n)} \quad (2)$$

wherein $\Gamma(n)$ is the gamma function. By constraining the step parameter to be one (n = 1; i.e., a single-step process), the fit to the experimental data was poor ($p < 0.0001$, chi-square test) (Figure 1D, red line). Therefore, we used our raw, unbinned catastrophe time data at 12 µM tubulin to calculate the maximum likelihood estimates for the gamma distribution parameters. The step parameter was 2.93 ± 0.29 (95% confidence interval) in 12 µM GTP-tubulin. The gamma distribution provided a reasonable fit to experimental data ($p > 0.04$, chi-square test), consistent with a multistep process.

To verify that our results are not an artifact of imaging or growth conditions, we performed several additional control experiments. First, to eliminate the possibility that aging is

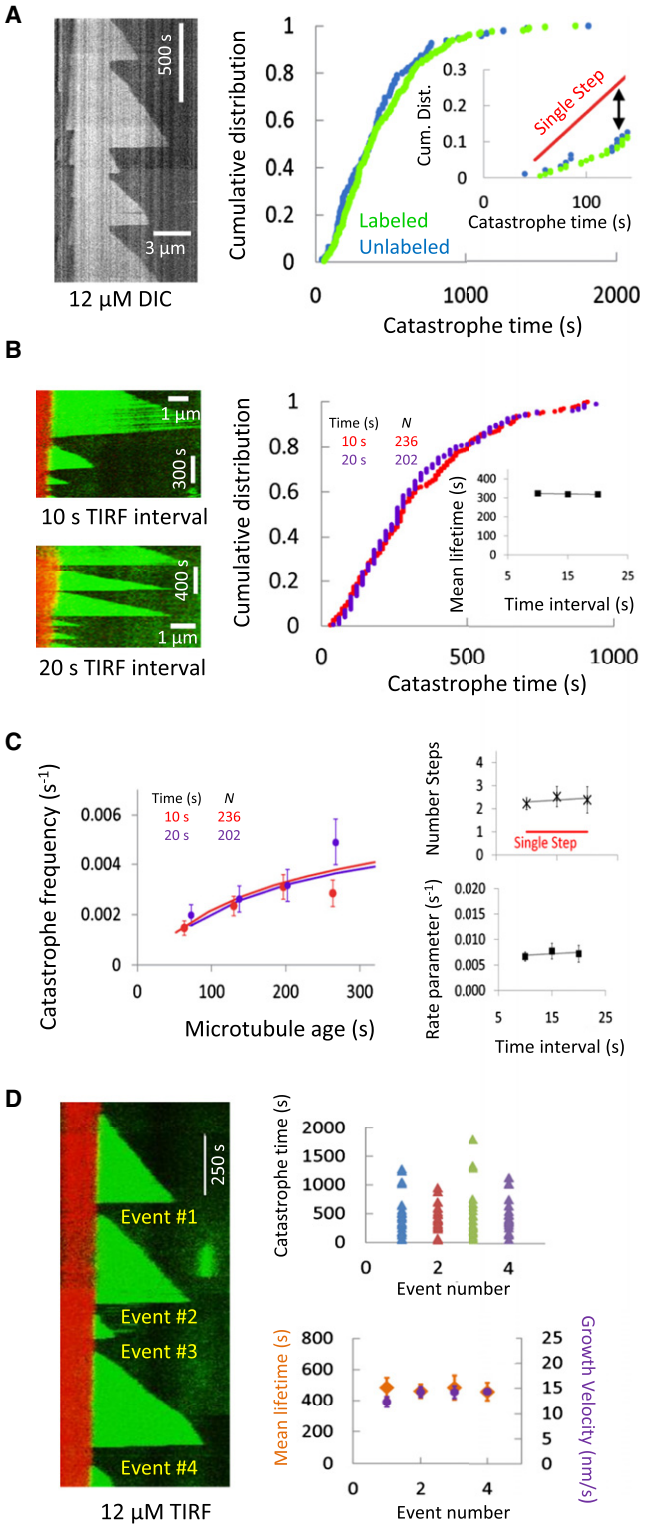

Figure 2. Controls against Light Damage and Rundown

(A) Control experiments with labeled and unlabeled tubulin were repeated using DIC microscopy (left, kymograph). Similar to the TIRF microscopy results, the catastrophe distribution at short times (right, inset), though expected to be linear for a single-step stochastic process (red line), is nonlinear due to fewer observed short time catastrophe events than predicted by a single-step process.

(B) To test whether light-induced damage occurs, we imaged growing microtubules using a series of longer time intervals (left). Regardless of the imaging time-lapse interval, the catastrophe time distributions were similar, with no significant effect of imaging frequency on the mean microtubule lifetimes (right).

(C) Regardless of time-lapse interval, the catastrophe frequency increases as a function of microtubule age (left). The gamma step and rate parameters are similar regardless of time-lapse interval (right). Error bars represent SE.

(D) Catastrophe times were analyzed as a function of the experimental chamber age (left). Both the mean microtubule lifetime and the mean microtubule growth velocity remained constant regardless of chamber age (right). See also Figure S3.

a result of light-induced damage during TIRF imaging, the 12 μM control experiments were repeated using differential interference contrast (DIC) microscopy (Figure 2A, left). Both labeled and unlabeled tubulin show a clear nonlinearity at early time points (Figure 2A, right, inset, green and blue dots) and fall well below the predicted constant catastrophe rate line (inset, red line). Therefore, the catastrophe frequency increases as a function of microtubule age in DIC, as was seen by TIRF microscopy (also see Figure S3).

Second, to further test that no light-induced damage occurs during TIRF imaging, we imaged growing microtubules at different time-lapse intervals. We found that, irrespective of whether the time-lapse interval was 10 s, 15 s, or 20 s (with the same exposure per frame), the catastrophe time distributions were similar, with no significant effect of total exposure on the mean microtubule lifetimes (Figure 2B). In addition, regardless of time-lapse interval, the catastrophe frequency increased as a function of microtubule age, suggesting that light-induced damage is not an important factor in the catastrophe of older microtubules (Figure 2C).

Finally, we analyzed catastrophes over a range of times after the beginning of an experiment, which is defined as the time that data collection is started (10 min after the tubulin is added to the experimental chamber). As shown in Figure 2D, both the mean lifetime and the mean growth velocity are independent of whether the microtubule is the first, second, third, or fourth to grow off the same seed. This demonstrates that catastrophe time does not depend on the age of the experimental chamber and also that our measurements represent steady-state conditions in the flow chamber. In addition, the free tubulin is not depleted during the experiments, as we calculate that, for an average extension length of 5 μm, the concentration of tubulin polymerized onto the seeds is ≈2.4 nM, which is less than one-thousandth the concentration of soluble tubulin used in the assays (7–14 μM; see Extended Experimental Procedures for calculations).

Thus, our data demonstrate that a catastrophe event results from at least three steps ($n \geq 3$) as the microtubule ages. This confirms earlier results based on smaller sample sizes (Odde et al., 1995).

Catastrophe Is a Multistep Process over a Range of Tubulin Concentrations

To test the generality of our finding, we repeated our measurements at tubulin concentrations ranging from 7 to 14 μM

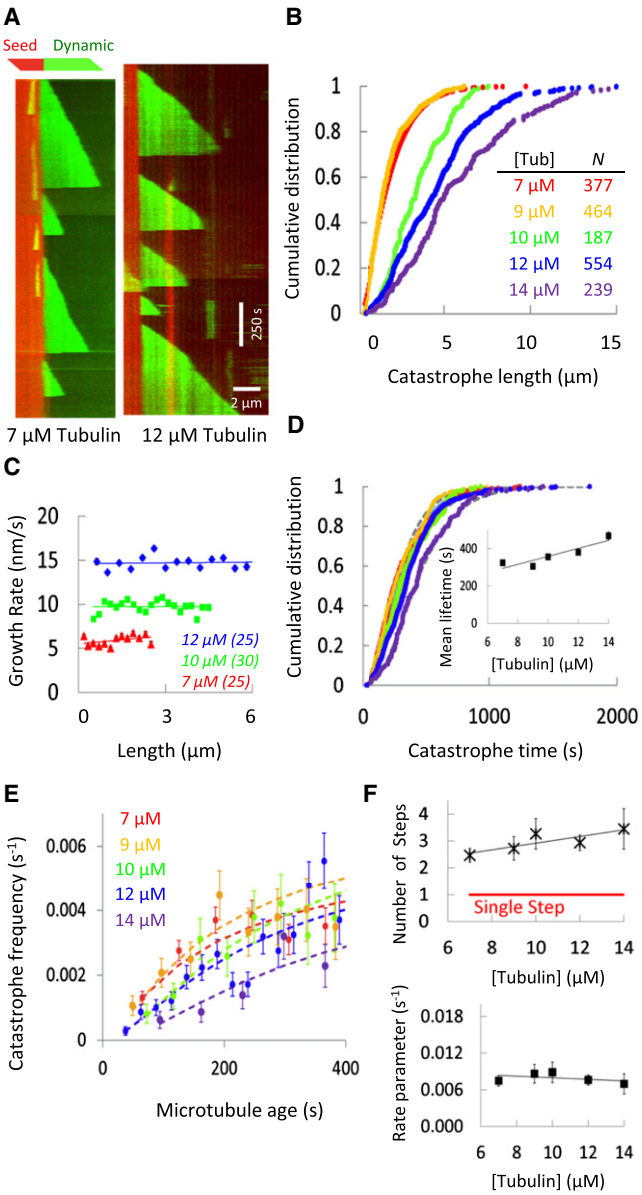

Figure 3. Catastrophe Depends on Microtubule Age over a Range of Tubulin Concentrations

(A and B) Catastrophe length distributions were independently measured and then plotted over a range of tubulin concentrations.

(C) The growth rate of microtubules was slower at lower tubulin concentrations and was independent of microtubule length.

(D) The effect of tubulin concentration on the catastrophe time was less pronounced than on catastrophe length (colors as in B). The inset shows that increasing the tubulin concentration leads to a small increase in the lifetime.

(E) Regardless of the tubulin concentration, the catastrophe frequency increased with microtubule age, consistent with a multistep catastrophe process (error bars = SE).

(F) Catastrophe is described by a multistep process (n > 1, top) over the observed range of tubulin concentrations. Tubulin concentration has only a mild influence on either of the gamma distribution parameters (error bars = 95% confidence intervals).

(Figure 3A). This range was chosen to minimize the number of missed catastrophe events so as not to bias the catastrophe length and time distributions. For example, below 7 μM, the microtubules tend to be short, and it is difficult to accurately measure the shortest ones. Above 14 μM, the microtubules tend to be long and to bend away from the surface (due to thermal fluctuations); it is difficult to accurately measure the longest ones in the TIRF assay. In addition, at high tubulin concentrations, the microtubules tend to grow out of the field of view of the camera (33 μm), and rescue events complicate the analysis. By restricting our analysis to 7–14 μM, we minimized these sources of experimental bias.

Increasing the tubulin concentration from 7 μM to 14 μM (Figure 3B) more than tripled the mean catastrophe length from 1.83 ± 0.08 μm (mean ± SE, n = 377) to 5.7 ± 0.22 μm (mean ± SE, n = 239). This large increase in catastrophe length correlated with the increased microtubule growth rates at higher tubulin concentrations (Figure 3C). Because the catastrophe time is approximately equal to the catastrophe length divided by the growth velocity, we expected that the effect of tubulin on the catastrophe time distribution would be less pronounced than on the catastrophe length distribution. This is indeed the case: the independently measured catastrophe time distribution curves nearly superimpose (Figure 3D), with only a small increase in mean lifetimes with increasing tubulin concentrations (Figure 3D, inset). This indicates that microtubule age is the dominant predictor of catastrophe, rather than length. For example, after 300 s of growth, microtubules in 12 μM GTP-tubulin are ~5 μm long on average, whereas in 7 μM GTP-tubulin, they are only ~2 μm on average. However, in both cases, ~50% of microtubules will catastrophe by this time.

The catastrophe frequency increased as a function of microtubule age, regardless of tubulin concentration (Figure 3E). We fit the multistep model to each catastrophe time raw data set (dashed gray curves in Figure 3D) and found that the number of steps increased slightly from 2.5 ± 0.26 at 7 μM tubulin (n = 608 microtubules, 95% confidence interval) to 3.4 ± 0.76 (n = 141 microtubules, 95% confidence interval) at 14 μM tubulin (Figure 3F, top). In all cases, the step parameter was significantly larger than 1 (Figure 3F, bottom) and therefore inconsistent with the single-step model. The effect of tubulin concentration on either the step parameter or the rate parameter was slight, consistent with our observation that tubulin concentration had only a small effect on catastrophe time over the range of concentrations that we tested.

Experimental Design for Testing Whether the Kinesins Are Catastrophe Factors

Having characterized catastrophes in tubulin alone, we asked whether the depolymerizing kinesins are catastrophe factors and, if they are, whether they alter the microtubule aging process. To quantify the kinesin effects, we added increasing concentrations of protein to flow cells containing 12 μM GTP-tubulin and measured the effect on the catastrophe length and catastrophe time distributions. In order to avoid biases introduced if the lengths or lifetimes become too long or short (and an appreciable number of events are missed), we restricted our study to Kip3 and MCAK concentrations that kept the

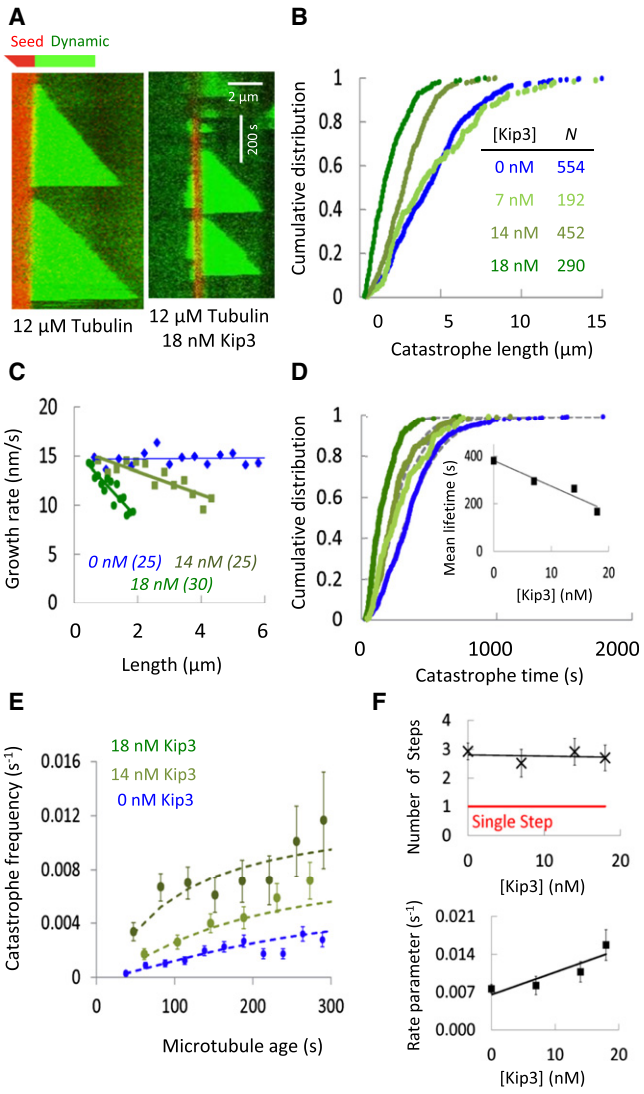

Figure 4. The Kinesin-8 Molecular Motor Kip3 Promotes Length-Dependent Slowing of Microtubule Growth and Accelerates the Rate of Microtubule Aging

(A) In the presence of Kip3 and 12 μM GTP-tubulin, green microtubules grow from red seeds.

(B) The cumulative catastrophe length distribution in various concentrations of Kip3.

(C) Kip3 promotes length-dependent slowing of microtubule growth rate, such that longer microtubules grow more slowly than shorter microtubules.

(D) Increasing concentrations of Kip3 in the presence of 12 μM tubulin (colors as in B) reduced the time to catastrophe and the mean microtubule lifetime (inset).

(E) Catastrophe frequency increased as a function of microtubule age in the presence of Kip3 (error bars = SE).

(F) Increasing concentrations of Kip3 led to an increase in the rate parameter for aging (*r*, bottom), whereas the minimum number of steps that are required to produce a catastrophe event (*n*, top) remained unchanged (error bars = 95% confidence intervals). Thus, Kip3 promotes catastrophe by accelerating the rate of microtubule aging.

catastrophe distributions within the range established for the different tubulin concentrations. In other words, we "bracketed" the kinesin concentrations by the tubulin concentrations.

The Kinesin-8 Kip3 Reduces Microtubule Catastrophe Length

To determine whether Kip3 is a catastrophe factor, we added varying amounts of Kip3 to the dynamic assay (Figure 4A). Kip3 reduced the catastrophe lengths relative to the 12 μM controls (Figure 4B). The mean catastrophe length was reduced more than 2-fold in 18 nM Kip3 to 1.81 ± 0.08 μm (mean ± SE, n = 290 microtubules) from 4.46 ± 0.11 μm (mean ± SE, n = 554) in the 12 μM control ($p < 0.0001$, t test). This is a similar decrease to that obtained when the tubulin concentration was reduced to 7 μM.

Kip3 Slows Microtubule Growth Rate in a Length-Dependent Fashion

The reduction in catastrophe length by Kip3 could be due to a decrease in growth rate, as seen when the tubulin concentration is reduced. Indeed, we found that Kip3 reduced the microtubule growth rate. However, in contrast to the effect of decreasing tubulin concentration (Figure 3C), the effect of Kip3 on microtubule growth rate depended on the extension length of the microtubule (Figure 4C): the growth rate of short microtubules was similar to that of controls, but the growth rate of long microtubules was decreased. This effect is consistent with a model in which longer microtubules more efficiently recruit Kip3 motors, leading to a higher flux of the processive Kip3 motors to the microtubule ends, where they reduce the growth rate (Varga et al., 2006, 2009).

Kip3 Reduces Microtubule Lifetimes

Because Kip3 promotes length-dependent slowing of microtubule growth, we expected that Kip3's effect on catastrophe time would be distinct from its effect on catastrophe length. Therefore, we measured catastrophe time over a range of Kip3 concentrations, all in the presence of 12 μM GTP-tubulin (Figure 4D). Although Kip3 had a more modest effect on the catastrophe time compared to its effect on the catastrophe length, increasing the Kip3 concentration nevertheless resulted in a large decrease in mean microtubule lifetimes (Figure 4D, inset). Thus, Kip3 is a catastrophe factor.

Kip3 Accelerates the Rate of Microtubule Aging that Leads to Catastrophe

To determine the mechanism by which Kip3 induces catastrophes, we calculated the dependence of catastrophe frequency on age (Figure 4E). The catastrophe frequency increases substantially with age, showing that, in the presence of Kip3, catastrophe remains a multistep process. We fit the multistep model to all of the raw catastrophe time data sets (dashed gray lines in Figure 4D) and found that the number of steps was significantly greater than one and was independent of the Kip3 concentration (slope of step parameter versus Kip3 concentration line: −0.004 ± 0.037, mean ± 95% CI) (Figure 4F, top). By contrast, the rate parameter (*r*) was larger at higher Kip3 concentrations, increasing ~2-fold at 18 nM Kip3 (Figure 4F, bottom,

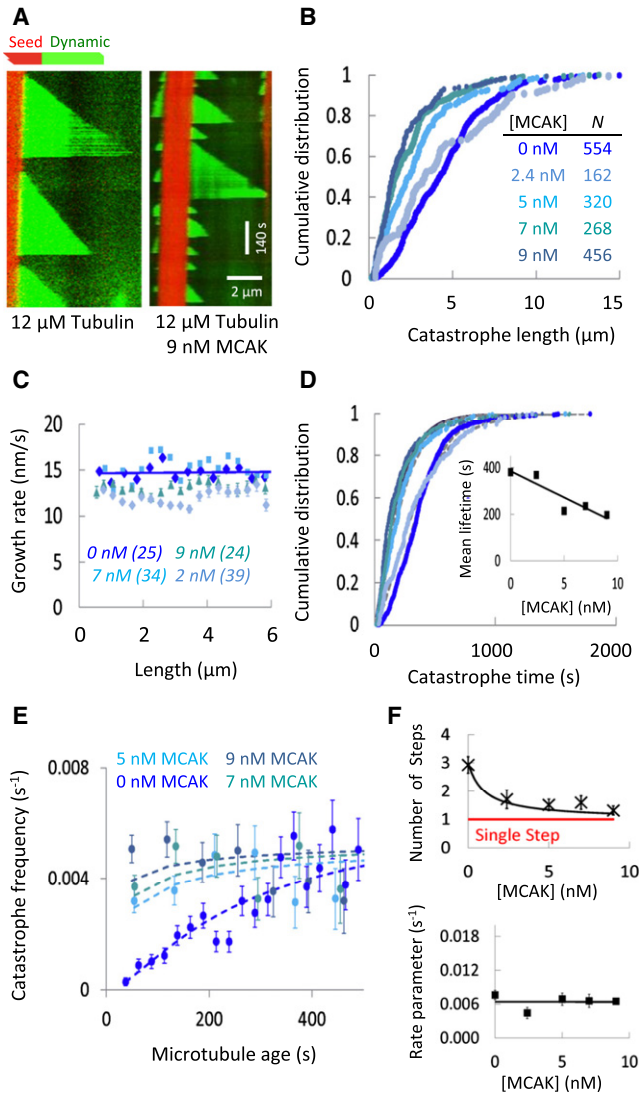

Figure 5. The Kinesin-13 Molecular Motor MCAK Eliminates the Aging Process that Leads to Catastrophe

(A) In the presence of MCAK and 12 μM GTP-tubulin, green microtubules grew from red seeds, and many catastrophes of short microtubules were observed.

(B) The cumulative catastrophe length distribution in various concentrations of MCAK.

(C) MCAK did not decrease microtubule growth rate as a function of length, and there was no apparent trend toward slower growth at higher MCAK concentrations.

(D) MCAK has a potent effect on the catastrophe time distribution (colors as in B) and reduced the mean microtubule lifetimes (inset).

(E) Regardless of MCAK concentration, the dependence of catastrophe frequency on microtubule age was reduced in the presence of MCAK (error bars = SE).

(F) Increased concentrations of MCAK led to a reduction in the number of catastrophe-promoting steps that are required to produce a catastrophe event (top), whereas the rate of acquiring catastrophe-promoting features remained relatively constant (bottom). Error bars represent 95% confidence intervals. See also Figure S4.

$p < 0.005$ by a t test). This suggests that Kip3 acts specifically to increase the rate of microtubule aging, thus increasing the catastrophe frequency and decreasing the microtubule lifetimes.

The Kinesin-13 MCAK Is a Catastrophe Factor

Like Kip3, the addition of MCAK to dynamic microtubules (Figure 5A) reduced catastrophe lengths as compared to control microtubules (Figure 5B). The average microtubule catastrophe length in 9 nM MCAK was 2.29 ± 0.10 μm (mean ± SE, n = 456 microtubules), similar to the average microtubule catastrophe length of 1.81 ± 0.08 μm observed in 18 nM Kip3.

MCAK does not reduce microtubule growth rates, consistent with a recent report (Montenegro Gouveia et al., 2010). Although the mean growth rate varied slightly for different concentrations of MCAK, there was no apparent trend toward slower growth at higher MCAK concentrations (Figure 5C). This is consistent with the low depolymerase activity of MCAK on GMPCPP-stabilized seeds under our experimental conditions (Figure S4). Furthermore, the growth rate was independent of microtubule length (Figure 5C), similar to control microtubules and in contrast with the length-dependent slowing of microtubule growth by Kip3.

The effect of MCAK on catastrophe time (Figure 5D) was qualitatively similar to its effect on catastrophe length, as expected because MCAK does not have a substantial influence on the microtubule growth rate. Like Kip3, MCAK strongly reduces the mean microtubule lifetime (Figure 5D, inset): MCAK is also a catastrophe factor.

MCAK Eliminates the Aging Process that Leads to Catastrophe

To determine the mechanism by which MCAK induces catastrophes, we calculated the dependence of catastrophe frequency on age (Figure 5E). Strikingly, MCAK altered the dependence of catastrophe frequency on microtubule age, such that catastrophe frequency was less dependent on microtubule age. Thus, in the presence of MCAK, there is not the paucity of short lifetimes observed in tubulin alone and in the presence of Kip3; the abundance of short microtubules in the presence of MCAK is obvious from the kymographs (compare Figure 5A to Figure 4A). This result suggests that catastrophe is not a multistep process in the presence of MCAK but, rather, that catastrophe depends on a single stochastic event at the microtubule end.

This conclusion was confirmed by fitting the gamma model to the raw catastrophe time data sets (Figure 5D, dashed gray lines). Whereas the rate parameter (r) remained relatively unchanged by MCAK (Figure 5F, bottom), the number of steps (n) decreased from 2.8 ± 0.17 (mean ± 95% CI) in the 12 μM tubulin controls to 1.31 ± 0.08 when 9 nM MCAK was added (Figure 5F, top). Thus, the number of steps required to initiate a catastrophe event is ~1 in MCAK, indicating that MCAK abolishes the aging process, in contrast to Kip3, which accelerates it.

DISCUSSION

We found that microtubule catastrophe is a multistep process. Because this finding is surprising and has important implications for the GTP cap model and for the measurement of catastrophe

frequency in vivo and in vitro, we performed several control experiments. First, we restricted our measurements to a relatively small range of tubulin and kinesin concentrations to minimize biases introduced by missing short and long events. Second, we confirmed that multistep catastrophes were not due to light damage. And third, the MCAK experiments served as an important control because they confirm that short events can indeed be detected.

We do not think that the paucity of catastrophes at short lengths is due to microtubule end proximity to the surface (the shorter the length, the closer to the seed and therefore the surface). This is because, in the absence of kinesins, microtubule age, and not length, is the primary predictor of catastrophe (compare Figures 3B and 3D). Furthermore, the high catastrophe rate at short lengths in the presence of MCAK also argues against a surface effect.

In addition to our own control experiments, two additional observations from the literature support the multistep mechanism of catastrophe. First, nonexponential cumulative catastrophe distributions have been reported by the Odde (Odde et al., 1995) and Dogterom (Janson et al., 2003) labs. And second, many labs have reported that the distribution of lengths in a population of dynamic microtubules deviates from the exponential predicted by single-step models (Stepanova et al., 2010; Tischer et al., 2009; Cassimeris et al., 1986; Du et al., 2010; Foethke et al., 2009; Fygenson et al., 1994; Voter et al., 1991; Walker et al., 1991). In these studies, the nonexponential length distributions provide support for the multistep process that does not rely on the direct observation of catastrophes. Taken together, the new results in this paper and the observations from the literature provide strong evidence that microtubule catastrophe is a multistep process, rather than a single-step process, as commonly assumed.

Another of our findings that contradicts a commonly held view is that the catastrophe frequency correlated only weakly with growth rate. First, we found that a 2-fold increase in tubulin concentration more than doubled the growth rate but only decreased the catastrophe frequency by ~25%. This finding is consistent with the results from Walker et al. (Walker et al., 1988) over a corresponding range of microtubule growth rates. However, they found that a further increase in tubulin concentration dramatically decreased the catastrophe frequency, a finding reported by several other groups (e.g., Chrétien et al., 1995). Also, lowering the tubulin concentration has been reported to dramatically increase the catastrophe rates (Chrétien et al., 1995; Voter et al., 1991; Walker et al., 1991). Second, MCAK had little effect on growth rate and yet had a dramatic effect on catastrophe frequency. Taken together with results from the literature (Fygenson et al., 1994), our results suggest that catastrophe is not simply related to growth.

Nature of the Microtubule Aging Process

Our picture of the multistep process is that catastrophe-promoting lattice features at the microtubule end are acquired and remembered as the microtubule ages. During growth, "destabilizing events" occur, and these events are remembered as structural features that increase the likelihood of catastrophe. After a sufficient number of these events, a catastrophe occurs. In other words, we think it is likely that the microtubule tip structure is evolving in a time-dependent fashion from a stable configuration when microtubules are young to a less stable configuration when microtubules have aged. The depolymerizing kinesins Kip3 and MCAK both increase the catastrophe frequency but by different mechanisms: Kip3 increases the rate of formation of lattice-destabilizing features, whereas MCAK reduces the number of features necessary for catastrophe.

Our finding that catastrophe depends on microtubule age has interesting implications for the GTP cap model because it suggests that the cap has substructure. We do not know what the catastrophe-promoting structural feature is. There are several possibilities. For example, the protofilaments might have individual caps, and catastrophe may occur when a minimum of three protofilaments become uncapped (Figure 6D). These uncapped protofilaments could be adjacent, or they could be separated from each other. This possibility requires that the uncapped protofilament remains as the microtubule grows; perhaps if the GTP hydrolyzes in the last subunit, hydrolysis of incoming subunits is accelerated. Another possibility is that the catastrophe-promoting feature is a structural dislocation of a protofilament relative to its neighbors. Again, the dislocation must be retained as the microtubule grows. Catastrophe would occur when three or more dislocations are accumulated. A third possibility is that the feature corresponds to loss of a protofilament at the microtubule tip; if enough protofilaments are lost, then the microtubule catastrophes. Changes in protofilament number have been observed by cryoelectron microscopy (Chrétien et al., 1992, 1995), but whether they correlate with microtubule age or catastrophe is not known. Changes in protofilament number could explain the presence of the GTP-tubulin "remnants" along the microtubule lattice, as described by Dimitrov et al. (2008), which would represent GTP-capped lagging protofilaments. The effects of the kinesins are compatible with all three possibilities. In the case of Kip3, the removal of subunits might increase the likelihood of exposure of a GDP subunit, the formation of a dislocation, or the loss of the protofilament. MCAK may have higher activity on GDP tubulin or a lattice dislocation. Clearly, additional experiments are required to test these and other possibilities.

The Mechanism of Catastrophe Promotion by Kip3 and MCAK

The increase in catastrophe frequency by Kip3 and MCAK is generally consistent with the idea that these proteins act by promoting the depolymerization of the growing GTP cap, thereby destabilizing it and increasing the likelihood that it is lost and the microtubule undergoes catastrophe. The alternative hypothesis, that Kip3 and MCAK act by slowing polymerization, is not readily reconciled with the data. For example, if Kip3 simply inhibits the subunit addition rate, then adding Kip3 should be equivalent to reducing the tubulin concentration; yet, the latter treatment has a much weaker effect on the catastrophe rate than addition of Kip3. Rather than inhibiting subunit addition, it appears instead that, by accelerating subunit removal from the microtubule tip, Kip3 increases the rate of formation of lattice-destabilizing features. Likewise, the finding that MCAK reduces the number of steps required for catastrophe suggests that it is

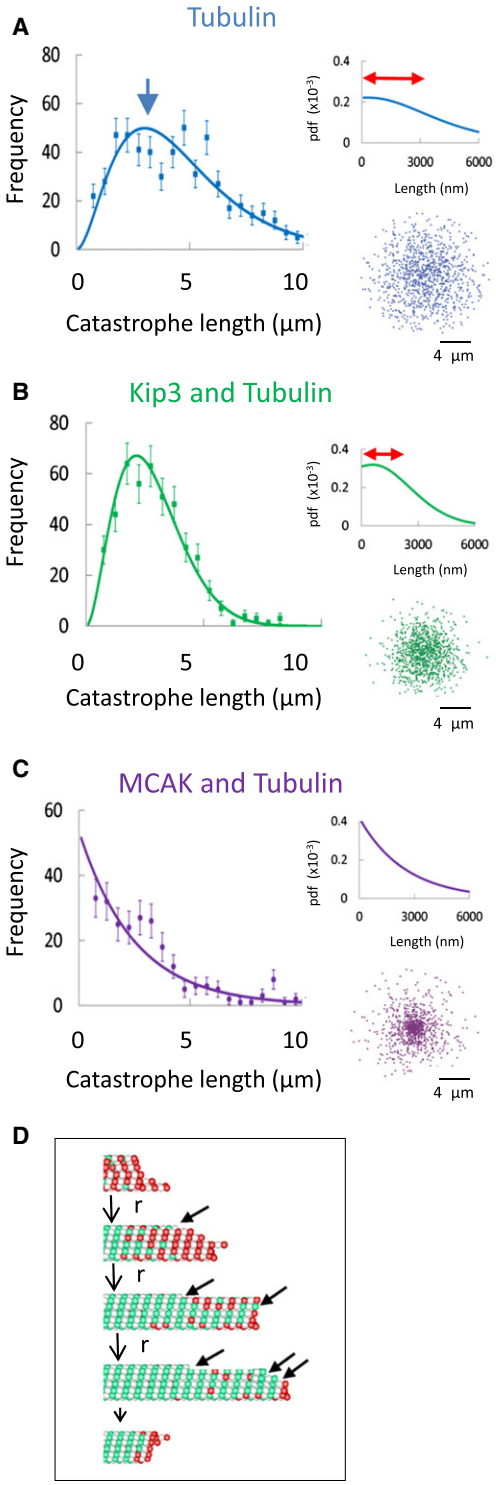

Figure 6. System-wide Microtubule Length Control by Depolymerizing Kinesins

(A) Because catastrophe requires multiple steps in tubulin alone, catastrophe events are less likely for shorter microtubules (left). As a result, microtubules shorter than the peak catastrophe length (blue arrow) will tend to grow well, creating a zone of high microtubule density that surrounds the microtubule nucleation origin (upper-right; pdf, probability density function in units of nm^{-1}; red double-arrow; see Extended Experimental Procedures for calculations). The theoretical density of catastrophe lengths around a nucleation point is shown in the lower right; each blue dot represents a catastrophe length.

(B) The addition of Kip3 results in a narrow distribution of microtubule catastrophe lengths (left; lower-right), creating a well-defined region of high microtubule density that is away from the microtubule nucleation origin (upper-right).

(C) Although MCAK is a potent catastrophe promoter, MCAK is not able to fine-tune the distribution of catastrophe lengths away from the nucleation origin (left), and as a result, microtubule catastrophe lengths (left; lower-right) and microtubule lengths (upper-right) are highly concentrated at the nucleation origin, regardless of MCAK concentration.

(D) Stochastic GDP-tubulin exposure at the tips of individual protofilaments may prevent efficient growth of these protofilaments, leading to lattice-destabilizing features that are remembered in time. Kip3 may act by increasing the rate of producing spontaneous protofilament uncapping events that ultimately lead to catastrophe, whereas MCAK could either create or stabilize curled protofilaments at the microtubule tip, thus destabilizing the entire microtubule tip.

not simply reducing the subunit on rate. Because MCAK does not increase the rate of lattice-destabilizing feature formation, it appears that MCAK recognizes the feature only after it has formed; only then does MCAK use the lattice-destabilizing feature as a starting point for destabilizing the entire cap, perhaps by inducing protofilament curling (Moores and Milligan, 2006; Mulder et al., 2009).

The Effect of Catastrophe Mechanism on Microtubule Length Distribution

What are the consequences of the different catastrophe mechanisms of the kinesins on the system-wide determination of microtubule lengths? In tubulin alone, the multistep process implies that microtubules are less likely to catastrophe when they are short (as compared to when they are long), creating a peak in the probability density function for microtubule catastrophe (Figure 6A, left, blue arrow). Therefore, microtubules that are shorter than the peak catastrophe length will tend to grow well, creating a zone of high microtubule density surrounding the microtubule nucleation origin (Figure 6A, upper-right, red double arrow; see Extended Experimental Procedures). This inherent property of microtubule catastrophe has a significant influence on the density of space exploration by microtubule tips, such that microtubule tip exploration can be concentrated in a dense zone away from the nucleation origin (Figure 6A, lower-right, blue dots represent individual microtubule catastrophe lengths for microtubules originating from the center). Thus, search and capture of kinetochores by dynamic microtubule tips could be regulated, in part, by a catastrophe mechanism that is inherent to the microtubule itself (Wollman et al., 2005).

The distribution of catastrophe lengths in 14 nM Kip3 shows that the most common catastrophe length is nearly equal to the mean catastrophe length, with a narrow range of catastrophe lengths both smaller and larger than the mean length (Figure 6B, left). Thus, the search space that a microtubule tip will explore in the presence of Kip3 occurs within a strongly limited zone of optimal microtubule growth while still allowing for robust search away from the nucleation origin (Figure 6B, upper-right, red

double arrow zone, and lower-right, where green dots represent catastrophe lengths). Because Kip3 leverages the natural tendency of microtubules to grow well when they are short but also limits longer microtubule lengths via length-dependent velocity slowing, this could explain, in part, why metaphase kinetochore oscillation amplitudes in human cells are larger and faster in the absence of the Kip3 homolog Kif18A (Jaqaman et al., 2010; Stumpff et al., 2008). Thus, though Kip3 is a relatively weak microtubule depolymerase, it has the unique ability to limit longer microtubule growth while still allowing for robust growth of shorter microtubules, thus concentrating microtubule tip excursions to a narrow region of space that is away from the nucleation origin.

In contrast, the catastrophe length distribution in 7 nM MCAK approximates an exponential distribution, in which the most common catastrophe length observed is in the shortest histogram bin, with a long tail of longer lengths observed as well (Figure 6C, left). Thus, although the mechanism for catastrophe promotion in Kip3 is optimized to produce a narrow microtubule catastrophe length distribution, MCAK results in a wider catastrophe length range. In this case, there is no optimal search zone outside of the nucleation area (Figure 6C, right). Rather, by reducing the number of steps that are required to promote a catastrophe event, MCAK is uniquely proficient in rapid catastrophe promotion. Therefore, MCAK is ideally suited for rapid restructuring in the cell, as could be mediated by a phosphorylation event, such as to break down a mitotic spindle at the completion of mitosis (Rankin and Wordeman, 2010) or to rapidly correct improper kinetochore-microtubule attachments during mitosis by synchronously promoting catastrophe of several microtubules (Bakhoum et al., 2009; Kline-Smith and Walczak, 2004; Wordeman et al., 2007).

Together, our results demonstrate how microtubule-associated proteins increase the versatility of microtubules in the cell. A protein such as Kip3 could be important when precise microtubule length control is required, such as during mitosis for spindle length control, during chromosome congression, or for efficient search and capture of kinetochores by microtubules (Du et al., 2010; Mayr et al., 2007; Stumpff et al., 2008; Wollman et al., 2005). In contrast, a potent catastrophe promoter such as MCAK would be better suited to allow for rapid depolymerization and restructuring of microtubules in the cell, such as during mitosis to correct improper kinetochore-microtubule attachments or to efficiently execute microtubule depolymerization and chromosome segregation during anaphase (Bakhoum et al., 2009; Goshima et al., 2005; Kline-Smith and Walczak, 2004; Rizk et al., 2009; Wordeman et al., 2007). Consistent with this division of labor between the depolymerizing kinesins, kinesin-13s, but not kinesin-8s, dramatically decrease the length of astral microtubules in the metaphase spindle, whereas kinesin-8s play a stronger role than kinesin-13s in regulating spindle length (Goshima et al., 2005).

EXPERIMENTAL PROCEDURES

TIRF Experiments

Assembly of GTP-tubulin labeled with Alexa-488 onto rhodamine-labeled GMPCPP-tubulin seeds was imaged by TIRF microscopy as previously described (Gell et al., 2010; Varga et al., 2006), with the exception that flow chambers were constructed with two layers of double-stick tape and with extra width to allow for longer time-lapse experiments without reaction chamber degradation. Images were collected with an Andor iXon camera on a Zeiss Axiovert 200 M microscope using a Zeiss100×/1.45 NA Plan FLUAR objective. The Imaging Buffer consisted of BRB80 supplemented with 40 mM glucose, 40 mg/ml glucose-oxidase, 16 mg/ml catalase, 0.1 mg/ml casein, and 10 mM DTT. In addition, all experiments included 1 mM GTP, 1 mM ATP, and 110 mM KCl, regardless of whether or not a motor was included in the assay. A 2.5× Optovar was used to provide additional magnification and to limit pixel size to ~64 nm. An objective heater was used to warm the flow channel to 28°C. In all cases, once reaction mixture was added to coverslip-attached seeds in the flow chamber, we waited 10 min prior to collecting images to allow the reaction to come to steady state.

Image Analysis

Image analysis was performed by creating kymographs of individual microtubule seeds, along with green extensions, using ImageJ analysis software. Catastrophe events are readily detected using this analysis, so catastrophe time can be measured using vertical distances, and catastrophe length can be measured using horizontal distances. Instant growth velocity was calculated for each 30 s interval, with the average length calculated for each interval. The growth rates versus time plots were calculated by binning length ranges together and then by calculating the mean and standard deviation of the instant growth velocity for each bin using MATLAB.

Gamma Distribution Fitting Analysis

Gamma distribution parameters were directly estimated using all experimental data (no binning) for catastrophe times or catastrophe lengths at a given experimental condition. Here, a gamma distribution was assumed, and the best-fit gamma model parameters were directly calculated from the entire catastrophe time data set for a given experimental condition. This was accomplished using the *gamfit* function in the MATLAB statistics toolbox, which calculates the maximum likelihood estimates (MLEs) and the corresponding confidence intervals for the parameters of the gamma distribution given the experimental data in an input vector.

SUPPLEMENTAL INFORMATION

Supplemental Information includes Extended Experimental Procedures and four figures and can be found with this article online at doi:10.1016/j.cell.2011.10.037.

ACKNOWLEDGMENTS

The authors thank members of the Howard Laboratory, in particular the Muffins Group, for advice and assistance. We thank Dr. V. Varga and Dr. C. Friel for protein and advice. M.K.G. was supported by a Whitaker International Scholar Fellowship, M.Z. by a Cross-Disciplinary Fellowship from the International Human Frontier Science Program Organization, and V.B. by a fellowship from the Boehringer Ingelheim Fonds.

Received: April 17, 2011
Revised: July 11, 2011
Accepted: October 26, 2011
Published: November 23, 2011

REFERENCES

Bakhoum, S.F., Genovese, G., and Compton, D.A. (2009). Deviant kinetochore microtubule dynamics underlie chromosomal instability. Curr. Biol. *19*, 1937–1942.

Caplow, M., and Shanks, J. (1996). Evidence that a single monolayer tubulin-GTP cap is both necessary and sufficient to stabilize microtubules. Mol. Biol. Cell *7*, 663–675.

Carlier, M.F., Hill, T.L., and Chen, Y. (1984). Interference of GTP hydrolysis in the mechanism of microtubule assembly: an experimental study. Proc. Natl. Acad. Sci. USA *81*, 771–775.

Cassimeris, L.U., Wadsworth, P., and Salmon, E.D. (1986). Dynamics of microtubule depolymerization in monocytes. J. Cell Biol. *102*, 2023–2032.

Chrétien, D., Metoz, F., Verde, F., Karsenti, E., and Wade, R.H. (1992). Lattice defects in microtubules: protofilament numbers vary within individual microtubules. J. Cell Biol. *117*, 1031–1040.

Chrétien, D., Fuller, S.D., and Karsenti, E. (1995). Structure of growing microtubule ends: two-dimensional sheets close into tubes at variable rates. J. Cell Biol. *129*, 1311–1328.

Desai, A., Verma, S., Mitchison, T.J., and Walczak, C.E. (1999). Kin I kinesins are microtubule-destabilizing enzymes. Cell *96*, 69–78.

Dimitrov, A., Quesnoit, M., Moutel, S., Cantaloube, I., Poüs, C., and Perez, F. (2008). Detection of GTP-tubulin conformation in vivo reveals a role for GTP remnants in microtubule rescues. Science *322*, 1353–1356.

Dogterom, M., Kerssemakers, J.W., Romet-Lemonne, G., and Janson, M.E. (2005). Force generation by dynamic microtubules. Curr. Opin. Cell Biol. *17*, 67–74.

Drechsel, D.N., and Kirschner, M.W. (1994). The minimum GTP cap required to stabilize microtubules. Curr. Biol. *4*, 1053–1061.

Du, Y., English, C.A., and Ohi, R. (2010). The kinesin-8 Kif18A dampens microtubule plus-end dynamics. Curr. Biol. *20*, 374–380.

Foethke, D., Makushok, T., Brunner, D., and Nédélec, F. (2009). Force- and length-dependent catastrophe activities explain interphase microtubule organization in fission yeast. Mol. Syst. Biol. *5*, 241.

Fygenson, D.K., Braun, E., and Libchaber, A. (1994). Phase diagram of microtubules. Phys. Rev. E Stat. Phys. Plasmas Fluids Relat. Interdiscip. Topics *50*, 1579–1588.

Gardner, M.K., Bouck, D.C., Paliulis, L.V., Meehl, J.B., O'Toole, E.T., Haase, J., Soubry, A., Joglekar, A.P., Winey, M., Salmon, E.D., et al. (2008). Chromosome congression by Kinesin-5 motor-mediated disassembly of longer kinetochore microtubules. Cell *135*, 894–906.

Gell, C., Bormuth, V., Brouhard, G.J., Cohen, D.N., Diez, S., Friel, C.T., Helenius, J., Nitzsche, B., Petzold, H., Ribbe, J., et al. (2010). Microtubule dynamics reconstituted in vitro and imaged by single-molecule fluorescence microscopy. Methods Cell Biol. *95*, 221–245.

Goshima, G., Wollman, R., Stuurman, N., Scholey, J.M., and Vale, R.D. (2005). Length control of the metaphase spindle. Curr. Biol. *15*, 1979–1988.

Gupta, M.L., Jr., Carvalho, P., Roof, D.M., and Pellman, D. (2006). Plus end-specific depolymerase activity of Kip3, a kinesin-8 protein, explains its role in positioning the yeast mitotic spindle. Nat. Cell Biol. *8*, 913–923.

Helenius, J., Brouhard, G., Kalaidzidis, Y., Diez, S., and Howard, J. (2006). The depolymerizing kinesin MCAK uses lattice diffusion to rapidly target microtubule ends. Nature *441*, 115–119.

Howard, J. (2001). Mechanics of Motor Proteins and the Cytoskeleton (Sunderland, MA: Sinauer Associates, Inc.).

Hunter, A.W., Caplow, M., Coy, D.L., Hancock, W.O., Diez, S., Wordeman, L., and Howard, J. (2003). The kinesin-related protein MCAK is a microtubule depolymerase that forms an ATP-hydrolyzing complex at microtubule ends. Mol. Cell *11*, 445–457.

Hyman, A.A., Salser, S., Drechsel, D.N., Unwin, N., and Mitchison, T.J. (1992). Role of GTP hydrolysis in microtubule dynamics: information from a slowly hydrolyzable analogue, GMPCPP. Mol. Biol. Cell *3*, 1155–1167.

Janson, M.E., de Dood, M.E., and Dogterom, M. (2003). Dynamic instability of microtubules is regulated by force. J. Cell Biol. *161*, 1029–1034.

Jaqaman, K., King, E.M., Amaro, A.C., Winter, J.R., Dorn, J.F., Elliott, H.L., McHedlishvili, N., McClelland, S.E., Porter, I.M., Posch, M., et al. (2010). Kinetochore alignment within the metaphase plate is regulated by centromere stiffness and microtubule depolymerases. J. Cell Biol. *188*, 665–679.

Kinoshita, K., Habermann, B., and Hyman, A.A. (2002). XMAP215: a key component of the dynamic microtubule cytoskeleton. Trends Cell Biol. *12*, 267–273.

Kline-Smith, S.L., and Walczak, C.E. (2002). The microtubule-destabilizing kinesin XKCM1 regulates microtubule dynamic instability in cells. Mol. Biol. Cell *13*, 2718–2731.

Kline-Smith, S.L., and Walczak, C.E. (2004). Mitotic spindle assembly and chromosome segregation: refocusing on microtubule dynamics. Mol. Cell *15*, 317–327.

Maney, T., Hunter, A.W., Wagenbach, M., and Wordeman, L. (1998). Mitotic centromere-associated kinesin is important for anaphase chromosome segregation. J. Cell Biol. *142*, 787–801.

Maurer, S.P., Bieling, P., Cope, J., Hoenger, A., and Surrey, T. (2011). GTPgammaS microtubules mimic the growing microtubule end structure recognized by end-binding proteins (EBs). Proc. Natl. Acad. Sci. USA *108*, 3988–3993.

Mayr, M.I., Hümmer, S., Bormann, J., Grüner, T., Adio, S., Woehlke, G., and Mayer, T.U. (2007). The human kinesin Kif18A is a motile microtubule depolymerase essential for chromosome congression. Curr. Biol. *17*, 488–498.

Mickey, B., and Howard, J. (1995). Rigidity of microtubules is increased by stabilizing agents. J. Cell Biol. *130*, 909–917.

Mitchison, T., and Kirschner, M. (1984). Dynamic instability of microtubule growth. Nature *312*, 237–242.

Montenegro Gouveia, S., Leslie, K., Kapitein, L.C., Buey, R.M., Grigoriev, I., Wagenbach, M., Smal, I., Meijering, E., Hoogenraad, C.C., Wordeman, L., et al. (2010). In vitro reconstitution of the functional interplay between MCAK and EB3 at microtubule plus ends. Curr. Biol. *20*, 1717–1722.

Moores, C.A., and Milligan, R.A. (2006). Lucky 13-microtubule depolymerisation by kinesin-13 motors. J. Cell Sci. *119*, 3905–3913.

Mulder, A.M., Glavis-Bloom, A., Moores, C.A., Wagenbach, M., Carragher, B., Wordeman, L., and Milligan, R.A. (2009). A new model for binding of kinesin 13 to curved microtubule protofilaments. J. Cell Biol. *185*, 51–57.

Newton, C.N., Wagenbach, M., Ovechkina, Y., Wordeman, L., and Wilson, L. (2004). MCAK, a Kin I kinesin, increases the catastrophe frequency of steady-state HeLa cell microtubules in an ATP-dependent manner in vitro. FEBS Lett. *572*, 80–84.

Nogales, E., and Wang, H.W. (2006). Structural mechanisms underlying nucleotide-dependent self-assembly of tubulin and its relatives. Curr. Opin. Struct. Biol. *16*, 221–229.

Nogales, E., Wolf, S.G., and Downing, K.H. (1998). Structure of the alpha beta tubulin dimer by electron crystallography. Nature *391*, 199–203.

Odde, D.J., Cassimeris, L., and Buettner, H.M. (1995). Kinetics of microtubule catastrophe assessed by probabilistic analysis. Biophys. J. *69*, 796–802.

Odde, D.J., Buettner, H.M., and Cassimeris, L. (1996). Spectral analysis of microtubule assembly dynamics. AIChE J. *42*, 1434–1442.

Phillips, R., Kondev, J., and Theriot, J. (2008). Physical Biology of the Cell (London: Taylor & Francis Group).

Rankin, K.E., and Wordeman, L. (2010). Long astral microtubules uncouple mitotic spindles from the cytokinetic furrow. J. Cell Biol. *190*, 35–43.

Rice, J.A. (1995). Mathematical Statistics and Data Analysis (Belmont, CA: Duxbury Press).

Rizk, R.S., Bohannon, K.P., Wetzel, L.A., Powers, J., Shaw, S.L., and Walczak, C.E. (2009). MCAK and paclitaxel have differential effects on spindle microtubule organization and dynamics. Mol. Biol. Cell *20*, 1639–1651.

Rogers, G.C., Rogers, S.L., Schwimmer, T.A., Ems-McClung, S.C., Walczak, C.E., Vale, R.D., Scholey, J.M., and Sharp, D.J. (2004). Two mitotic kinesins cooperate to drive sister chromatid separation during anaphase. Nature *427*, 364–370.

Stepanova, T., Smal, I., van Haren, J., Akinci, U., Liu, Z., Miedema, M., Limpens, R., van Ham, M., van der Reijden, M., Poot, R., et al. (2010). History-dependent catastrophes regulate axonal microtubule behavior. Curr. Biol. *20*, 1023–1028.

Stumpff, J., von Dassow, G., Wagenbach, M., Asbury, C., and Wordeman, L. (2008). The kinesin-8 motor Kif18A suppresses kinetochore movements to control mitotic chromosome alignment. Dev. Cell *14*, 252–262.

Tischer, C., Brunner, D., and Dogterom, M. (2009). Force- and kinesin-8-dependent effects in the spatial regulation of fission yeast microtubule dynamics. Mol. Syst. Biol. *5*, 250.

Tournebize, R., Popov, A., Kinoshita, K., Ashford, A.J., Rybina, S., Pozniakovsky, A., Mayer, T.U., Walczak, C.E., Karsenti, E., and Hyman, A.A. (2000). Control of microtubule dynamics by the antagonistic activities of XMAP215 and XKCM1 in Xenopus egg extracts. Nat. Cell Biol. *2*, 13–19.

Varga, V., Helenius, J., Tanaka, K., Hyman, A.A., Tanaka, T.U., and Howard, J. (2006). Yeast kinesin-8 depolymerizes microtubules in a length-dependent manner. Nat. Cell Biol. *8*, 957–962.

Varga, V., Leduc, C., Bormuth, V., Diez, S., and Howard, J. (2009). Kinesin-8 motors act cooperatively to mediate length-dependent microtubule depolymerization. Cell *138*, 1174–1183.

Voter, W.A., O'Brien, E.T., and Erickson, H.P. (1991). Dilution-induced disassembly of microtubules: relation to dynamic instability and the GTP cap. Cell Motil. Cytoskeleton *18*, 55–62.

Walczak, C.E., Mitchison, T.J., and Desai, A. (1996). XKCM1: a Xenopus kinesin-related protein that regulates microtubule dynamics during mitotic spindle assembly. Cell *84*, 37–47.

Walker, R.A., O'Brien, E.T., Pryer, N.K., Soboeiro, M.F., Voter, W.A., Erickson, H.P., and Salmon, E.D. (1988). Dynamic instability of individual microtubules analyzed by video light microscopy: rate constants and transition frequencies. J. Cell Biol. *107*, 1437–1448.

Walker, R.A., Inoué, S., and Salmon, E.D. (1989). Asymmetric behavior of severed microtubule ends after ultraviolet-microbeam irradiation of individual microtubules in vitro. J. Cell Biol. *108*, 931–937.

Walker, R.A., Pryer, N.K., and Salmon, E.D. (1991). Dilution of individual microtubules observed in real time in vitro: evidence that cap size is small and independent of elongation rate. J. Cell Biol. *114*, 73–81.

Wargacki, M.M., Tay, J.C., Muller, E.G., Asbury, C.L., and Davis, T.N. (2010). Kip3, the yeast kinesin-8, is required for clustering of kinetochores at metaphase. Cell Cycle *9*, 2581–2588.

Wollman, R., Cytrynbaum, E.N., Jones, J.T., Meyer, T., Scholey, J.M., and Mogilner, A. (2005). Efficient chromosome capture requires a bias in the 'search-and-capture' process during mitotic-spindle assembly. Curr. Biol. *15*, 828–832.

Wordeman, L., Wagenbach, M., and von Dassow, G. (2007). MCAK facilitates chromosome movement by promoting kinetochore microtubule turnover. J. Cell Biol. *179*, 869–879.

Zanic, M., Stear, J.H., Hyman, A.A., and Howard, J. (2009). EB1 recognizes the nucleotide state of tubulin in the microtubule lattice. PLoS ONE *4*, e7585.